대한기계학회 2021년 학술대회 KSME21-Th17A-026

Design and development of wall cleaning robot with dual rope climbing mechanism

Hobyeong Chae*†, Yecheol Moon*, Kyung Ook Lee*, Sung Jun Park*, Hwa Soo Kim**, TaeWon Seo*,
* Dept. of Mechanical Engineering, Hanyang Univ., * Dept. of Mechancial System Design the Kyonggi Univ.

Key Words: Wall cleaning robot, Rope climbing robot, Parallel kinematics

Abstract

Cleaning task for vertical structure, such as walls on buildings and construction sites, has a high risk of fall accident. For this reason, research on automation of wall cleaning task based on robotics technology has been actively conducted in recent years. However, wall cleaning robots developed in many studies either had limited mobility performance or need external infrastructure for operation. In this research, we designed and developed a novel wall cleaning robot which has two main contributions. First, locomotion in both vertical and horizontal direction on the wall is possible by controlling the two rope climbing mechanisms in parallel. Second, no external infrastructures like winch and gondola are required for the operation except for fixed rope. The prototype of robot was developed, and field tests were conducted to verify cleaning performance using image processing.

1. INTRODUCTION

Through the application of robot technology across many industries, safety problems have been solved and work efficiency has been increased. The wall cleaning robot is one of these applications. In the past, human workers used ladders or ropes to clean the walls, which has an extremely high risk of falling. Safety issues can be solved by automating the wall cleaning tasks using robots. Therefore, many studies have recently been conducted on wall cleaning robots and various commercial and research models have been developed.

For example, SERBOT's GEKKO [1], Zhang et al.'s sky cleaner [2], Qian et al's Dual Suction Cups [3] are equipped with vacuum suction autonomous mobile platform for locomotion. Kim et al's Rope Ride [4], Manntech's façade cleaning [5] and Schraft et al's SFRII [6] control vertical position by winch-controlled wire ropes. Wang et al's Skyboy [7] has magnetic attachment mechanism for locomotion. The model M1 developed in our previous studies can move in vertical direction via using building's gondola system [8]. Meanwhile, a study was also conducted to classify various wall cleaning robots and compare their performance [9].

However, existing wall cleaning robots have several limitations. The suction cup or magnetic attachment method can only be used for limited surface materials and have low movement speed. Wire winch or gondola type robots cannot move in horizontal direction without relocation of the wire, and external infrastructure is required. In this study, we developed a new wall cleaning robot that combines the advantages of existing models and its two main contributions are as follows.

First, the parallel control of the dual rope climbing mechanism allows free movement in both horizontal and vertical directions on the wall.

Second, installation of external infrastructures like electric wire winch of gondola system is unnecessary, and it can be used on any kind of wall with simply fixing a pair of rope. The rest of this paper consists of as follows. Sec.2 describes locomotion strategies of the proposed robot. Sec3 describes prototyping and experiments of the robot. Sec.4 summarizes conclusion and future research plans.

2. LOCOMOTION STRATEGIES

2.1 Parallel kinematics for motion control

The Parallel kinematics are designed to implement the robot's two degrees of freedom motion. Fig.1 represents the proposed robot hang on a pair rope, indicating its position, the length and angle of the rope.

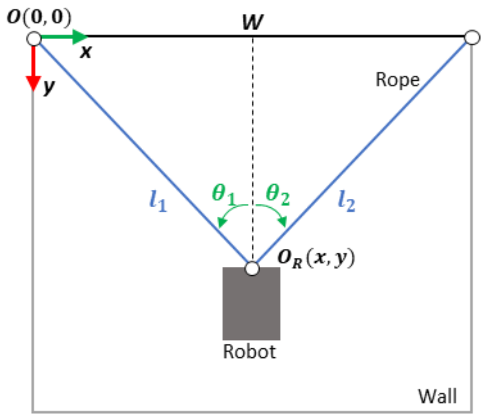

Fig.1 Kinematic diagram of the proposed robot.

Where O, O_R are workspace origin and coordinate of the robot, l_1, l_2 are length of left and right ropes, θ_1, θ_2 are angle between vertical line and the ropes, W is distance between rope fixing points on the wall.

The climbing mechanism of the robot adjusts the length of each ropes (l_1, l_2). To control the robot's velocity in cartesian coordinate system $(\dot{x}, \dot{y})$ by controlling rope length, it is necessary to obtain Jacobian matrix through differentiation of the constraint equations. The Jacobian matrix is a function of the rope angle (θ_1, θ_2). Relation between velocity, rope length and angle are shown in the equation below.

† Presenting Author, ppwerter21@hanyang.ac.kr

$$\begin{bmatrix} \dot{l}_1 \\ \dot{l}_2 \end{bmatrix} = J \begin{bmatrix} \dot{x} \\ \dot{y} \end{bmatrix} \quad (1)$$

Where $\dot{l}_1$, $\dot{l}_2$ are differentiation of each rope length, J is Jacobian matrix, $\dot{x}$ and $\dot{y}$ is robot's velocity in cartesian coordinate system. A more specific form of Jacobian matrix is shown in following equations.

$$J = J_2 J_1^{-1} \quad (2)$$

$$J_1 = W \begin{bmatrix} \frac{sec^2\theta_1 tan\theta_2}{(tan\theta_1+tan\theta_2)^2} & \frac{-sec^2\theta_2 tan\theta_1}{(tan\theta_1+tan\theta_2)^2} \\ \frac{-sec^2\theta_1}{(tan\theta_1+tan\theta_2)^2} & \frac{-sec^2\theta_2}{(tan\theta_1+tan\theta_2)^2} \end{bmatrix} \quad (3)$$

$$J_2 = W \begin{bmatrix} \frac{-cos\theta_2 \cos(\theta_1+\theta_2)}{sin^2(\theta_1+\theta_2)} & \frac{-cos\theta_2 \cos(\theta_1+\theta_2) - sin\theta_2 \sin(\theta_1+\theta_2)}{sin^2(\theta_1+\theta_2)} \\ \frac{-cos\theta_1 \cos(\theta_1+\theta_2) - sin\theta_1 \sin(\theta_1+\theta_2)}{sin^2(\theta_1+\theta_2)} & \frac{-cos\theta_1 \cos(\theta_1+\theta_2)}{sin^2(\theta_1+\theta_2)} \end{bmatrix} \quad (4)$$

2.2 Rope climbing mechanism

The rope climbing capability has been implemented by an endless rope winch mechanism with Capstan principle. Fig.2 describes the structure of the mechanism and the forces acting on it.

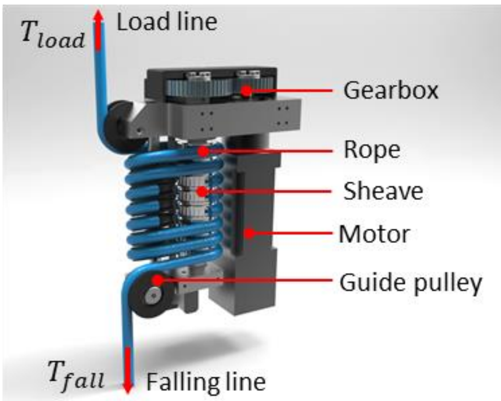

Fig.2 Structure of the endless winch type rope climbing mechanism. The rope is wound eight times around the sheave and is pulled or released by frictional force. Torque is transferred by motor and gearbox.

The rope can be pulled or released by rotating the multistage rope sheave using servo motor. Meanwhile, the Capstan equation below shows the relationship between the tensile force and the frictional force at both ends of the rope wound around the sheave to prevent rope slip.

$$T_{fall} \geq \frac{T_{load}}{e^{\mu_k \theta}} \quad (5)$$

Where T_{fall} and T_{load} are tension on falling line and load line respectively, μ_k is kinetic friction coefficient between rope and sheave, θ is total wound angle of rope.

The equation must be satisfied for prevention of rope slip which results in bad motion control performance. Based on the actual design variables of the robot and experimental data, minimum falling line tension has been decided. Variables are summarized in Table 1.

Table 1 Variables for capstan equation

Symbol	Value	Unit	Remark
T_{load}	679	N	Total mass: 60Kg Acceleration: 1.5m/s2
μ_k	0.14	-	Experimental data
θ	25.1	rad	8 times wound with half contact angle
T_{fall}	20.1	N	Required falling line tension

3. EXPERIMENT AND RESULT

3.1 Prototype and experimental setup

Prototype model was developed to verify robot's operation and cleaning performance through field experiments. In addition to the climbing mechanism described in Sec.2, subsystems such as rope angle measurement sensors, waterproof main controller enclosures, and angle adjustable high-pressure nozzles were developed and integrated into a cleaning robot system. The configuration and operation example of the prototype model are described in Figure 3, and applied electronic components are listed in Table 2.

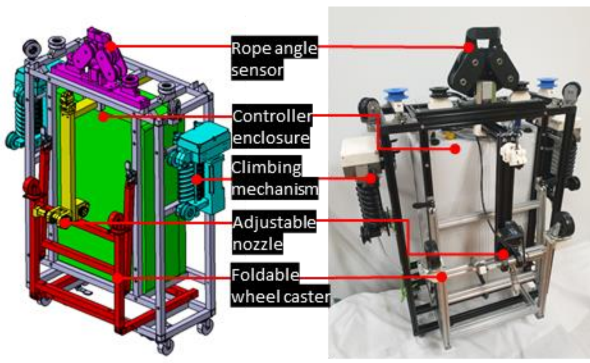

Fig.3 Configuration of the prototype including CAD modeling.

Table 2 Electronic components list

Component	Purpose	Manufacturer	Model
BLDC servo motor	Climbing mechanism	Maxon	IDX56L
FPGA Realtime controller	Main controller	National Instruments	cRIO-9042 w/ NI-9401
Magnetic absolute encoder	Rope angle measurement	RLS	MB039
Waterproof servo motor	Nozzle angle control	Sea LAB	D30

The field experiments were conducted on a concrete wall of a real-world building with size of 8m width and 10m height. Only a pair of rope were installed without any additional infrastructure. For the cleaning performance experiments, green colored pigment was used for artificial contamination of the wall. Experimental setup is described in Fig.4.

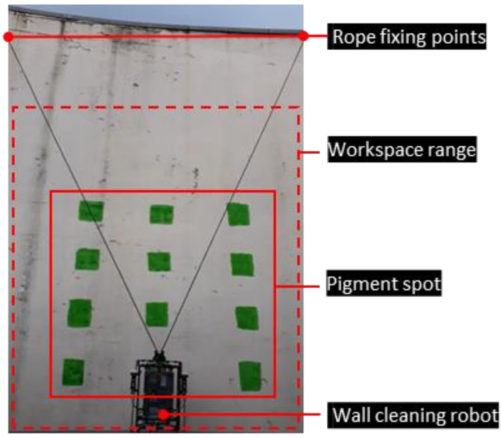

Fig. 4 Experimental setup where prototype of the wall cleaning robot was hung on a pair of fixed rope and green colored pigment spots were arranged in grid shape to implement contamination condition of the wall.

3.2 Mobility Test

To verify the mobility performance of the robot, the ascending velocity has been measured. Also, the robot moved toward arbitrary trajectory with cleaning the randomly placed pigment spots. As shown in Fig.5, the robot can achieve an ascending speed of up to 0.5 m/s. Also, it can move toward any location on the wall with various desired speed. The data comparing the ascending speed with other cleaning robot models are summarized in Table.3.

Table 3 ascending speed comparison from other models.

Model	Locomotion	Absolute speed [cm/s]	Body length /s
Gekko façade [1]	Suction	13	0.107
Sky cleaner [2]	Suction	3.5	0.245
Dual suction cup [3]	Suction	3.5	0.02
Rope ride [4]	Rope/Wire	25.5	0.175
Façade cleaning [5]	Rope/Wire	5.5	0.015
SFRII [6]	Rope/Wire	2	0.02
Skyboy [7]	Rope/Wire	18.5	0.14
FCR M1 [8]	Attached on gondola	12	0.3
Proposed model	**Rope/Wire**	**50**	**0.45**

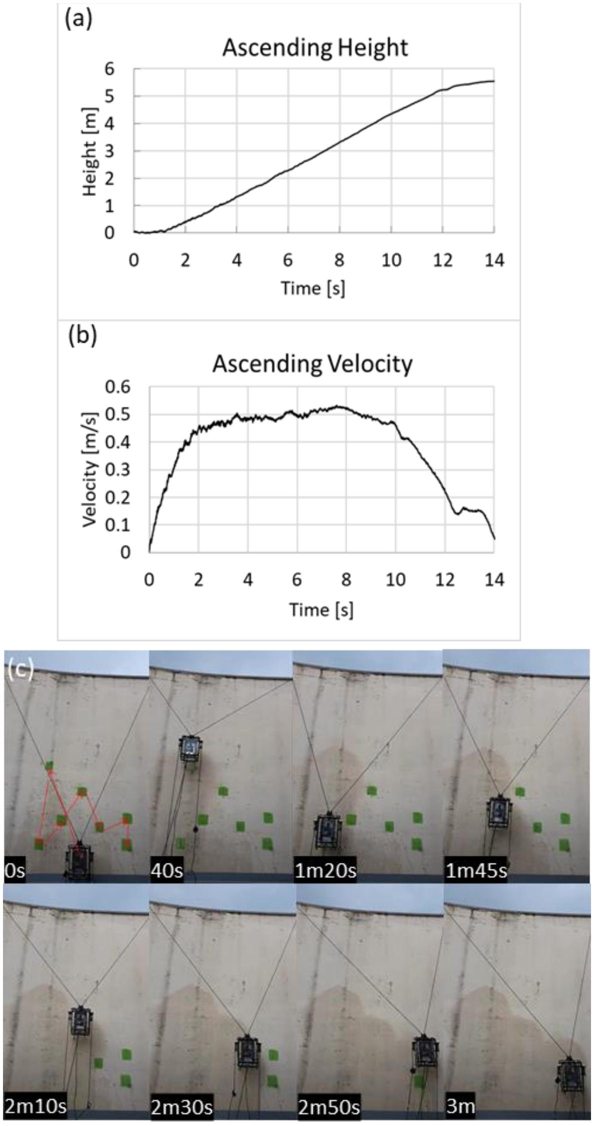

Fig.5 Experimental data from mobility tests. Ascending height (a) and velocity (b) has been plotted where maximum velocity reached around 0.5m/s while moving 5.5m. (c) shows photos of cleaning procedure with time stamps. Randomly scattered six spots were cleaned within 3 minutes.

3.3 Cleaning Test

To verify the cleaning performance of the robot, the contaminant spots arranged in grid patterns were cleaned using high-pressure spraying nozzle. The images of before and after the cleaning have been numerically analyzed through image processing. The analysis used CIELAB color space [10], which is very similar to human eye's color recognition. Higher A values represent intensity of red and lower values represent green. Similarly, B values represent intensity of yellow and blue. Three images of cleaning process were prepared, and average LAB values were calculated and normalized using image color summarizer [11]. The color difference value that can be used as a contamination index is obtained by measuring distance between LAB color map coordinates. The results are organized in Fig.6. If the contamination index of image 2 is considered as 100%, it can be confirmed that approximately 78% of the contamination was removed after a cycle of cleaning process.

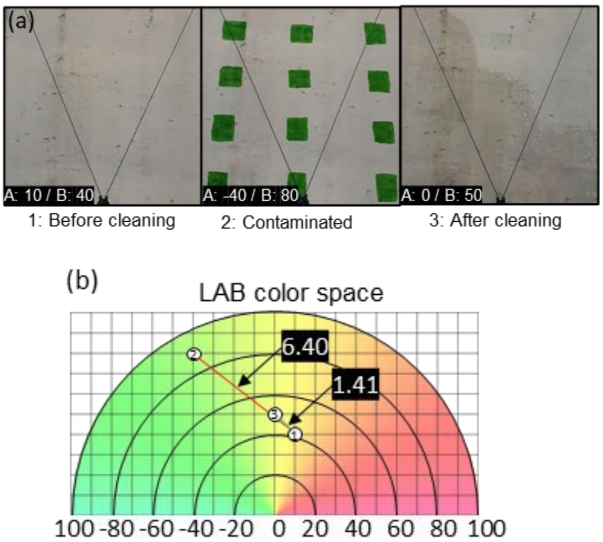

Fig.6 Experimental data from cleaning tests. Three images from cleaning experiment and A and B values are shown in (a). Coordinates and color difference values of each images are shown in (b).

4. CONCLUSION

As a result, we developed a wall cleaning robot which has high ascending speed and mobility and easy operation characteristics. Also, we verified its performance through field experiments. As a future research plan, we will develop advanced control techniques for vibration reduction and obstacle overcoming.

ACKNOWLEDGEMENT

This research was supported by the National Research Foundation of Korea(NRF) Grant funded by the Ministry of Science and ICT for First-Mover Program for Accelerating Disruptive Technology Development(NRF-2018M3C1B9088328). Corresponding authors (Hwa Soo Kim and TaeWon Seo)

REFERENCES

(1) SERBOT. GEKKO Facade Robot. Accessed: Aug. 31, 2021. [Online]. Available: https://www.serbot.ch/en/facades-surfaces-cleaning/gekko-facade-robot

(2) Zhang, H., Zhang, J., Wang, W., Liu, R., & Zong, G. (2007). "A series of pneumatic glass-wall cleaning robots for high-rise buildings. Industrial Robot: An International Journal, 34(2), 150–160.

(3) Qian, Z., Zhao, Y., Fu, Z., & Cao, Q. (2006). Design and realization of a non-actuated glass-curtain wall-cleaning robot prototype with dual suction cups. International Journal of Advanced Manufacturing Technology, 30, 147–155.

(4) Kim, T., Kim, J., Seo, K., Kim, H., Lee, G., Kim, J., et al. (2014). Design and control of a cleaning unit for a novel wall-climbing robot. Applied Mechanics and Materials, 541–542, 1092–1096.

(5) Manntech. (2021). Façade cleaning systems. https://www.manntech.com/solutions/(retrieved at Aug. 31, 2021)

(6) Schraft, R. D., Brauning, U., Orlowski, T., & Hornemann, M. (2000). Automated cleaning of windows on standard facades. Automation in Construction, 9, 489–501.

(7) Wang, W., Tang, B., Zhang, H., & Zong, G. (2010). Robotic cleaning system for glass facade of high-rise airport control tower. Industrial Robot: An International Journal, 37(5), 469–478.

(8) H. Chae *et al.*, "Façade Cleaning Robot With Manipulating and Sensing Devices Equipped on a Gondola," *IEEE/ASME Transactions on Mechatronics*, vol. 26, no. 4, pp. 1719–1727, Aug. 2021.

(9) T. Seo, Y. Jeon, C. Park, and J. Kim, "Survey on Glass And Façade-Cleaning Robots: Climbing Mechanisms, Cleaning Methods, and Applications," *International Journal of Precision Engineering and Manufacturing-Green Technology*, vol. 6, no. 2, pp. 367–376, Mar. 2019.

(10) P. R. Narkhede and A. V. Gokhale, "Color image segmentation using edge detection and seeded region growing approach for CIELab and HSV color spaces," in *2015 International Conference on Industrial Instrumentation and Control (ICIC)*, 2015.

(11) Image Color summarizer. Accessed: Aug. 31, 2021. [Online]. Available: http://mkweb.bcgsc.ca/color-summarizer/?analyze